JCB Report

Macrophage podosomes assemble at the leading lamella by growth and fragmentation

James G. Evans,[1,2] Ivan Correia,[2] Olga Krasavina,[2] Nicki Watson,[2] and Paul Matsudaira[1,2,3]

[1]BioImaging Center, [2]Whitehead Institute for Biomedical Research, Cambridge, MA 02142
[3]Department of Biology and Division of Biological Engineering, Massachusetts Institute of Technology, Cambridge, MA 02139

Podosomes are actin- and fimbrin-containing adhesions at the leading edge of macrophages. In cells transfected with β-actin–ECFP and L-fimbrin–EYFP, quantitative four-dimensional microscopy of podosome assembly shows that new adhesions arise at the cell periphery by one of two mechanisms; de novo podosome assembly, or fission of a precursor podosome into daughter podosomes. The large podosome cluster precursor also appears to be an adhesion structure; it contains actin, fimbrin, integrin, and is in close apposition to the substratum. Microtubule inhibitors paclitaxel and demecolcine inhibit the turnover and polarized formation of podosomes, but not the turnover rate of actin in these structures. Because daughter podosomes and podosome cluster precursors are preferentially located at the leading edge, they may play a critical role in continually generating new sites of cell adhesion.

Introduction

As a cell crawls forward, two distinct actin-based processes, protrusion of the leading edge and adhesion to the substratum, are coordinated in the lamella and coupled with actomyosin-mediated contraction of the cell body (Lauffenburger and Horwitz, 1996). Under control of Rho family GTPases and actin sequestering, capping, and branching proteins, polymerization of a branched actin network provides force for membrane protrusion (Ridley et al., 1992; Geiger and Bershadsky, 2001). An early step in the maturation of a nascent adhesion (focal complex) into a long-lived focal adhesion is the recruitment of integrin-associated signaling and cytoskeletal proteins to the smaller, short-lived focal complex (Beningo et al., 2001). Although focal adhesions may couple actomyosin-based contractility to the substratum via an integrin-mediated molecular clutch mechanism (Smilenov et al., 1999), force-mapping studies reveal that focal complexes located at the leading edge of the lamella generate stronger traction forces than larger elongated focal adhesions (Beningo et al., 2001). Although the composition and organization of focal adhesions is an area of intense study, relatively little is known about how the short-lived focal complexes transiently assemble in the leading lamella.

The macrophage is a model cell for studying the structure and dynamics of short-lived adhesions. Macrophages, like other monocyte-derived and RSV- or Src-transformed cells, adhere to the substratum through short-lived punctate adhesions called podosomes that are biochemically and structurally similar to focal complexes (Marchisio et al., 1987; Babb et al., 1997; Correia et al., 1999; Mizutani et al., 2002). Podosomes and focal complexes contain not only the same major cytoskeletal and membrane proteins including actin, integrins, vinculin, and talin (Geiger et al., 1984; Marchisio et al., 1988; Zamir et al., 2000), but also contain common signaling and scaffolding proteins including Ena/VASP (Reinhard et al., 1992), FAK/Pyk2, and paxillin (Volberg et al., 1995; Pfaff and Jurdic, 2001). Mutation of the Wiskott-Aldrich syndrome protein (Volkman et al., 2002) disrupts podosomes and impairs motility and function of monocyte-derived cells (Linder et al., 1999). Podosomes and focal complexes also turn over quickly in the leading lamella, suggesting a mechanism for coupling assembly with disassembly. Implicated in the assembly of cell adhesions are not only integrin receptors and actin, but also microtubules (Babb et al., 1997; Elbaum et al., 1999; Kaverina et al., 1999; Linder et al., 2000). Microtubules affect adhesion and the direction of cell movement by modulating the stability of cell adhesions and other actin-rich structures through Rho GTPases (Elbaum et al., 1999; Kaverina et al., 1999).

Although focal adhesions at the ends of stress fibers assemble de novo from clusters of integrin receptors (Smilenov et al., 1999), a fundamental question remains how focal complexes and podosomes assemble. To understand how cell adhesions

The online version of this article includes supplemental material.

Address correspondence to James G. Evans, Whitehead Institute, 9 Cambridge Center, Cambridge, MA 02142. Tel.: (617) 324-0300. Fax: (617) 258-7226. E-mail: jgevans@wi.mit.edu

Key words: fluorescence microscopy; adhesion; microtubules; actin; kymography.

continually assemble at the front of a cell, we GFP-tagged two major structural proteins of podosomes, β-actin and L-fimbrin, and perturbed their assembly with microtubule inhibitors. Quantitative four-dimensional (4-D)* microscopy of the leading edge of IC-21 macrophages revealed that podosomes, like the dendritic actin network in the leading lamella, assemble by a pattern of polarized growth and branching. Although some podosomes arise de novo, at the leading edge the majority assemble from older podosomes or, more dramatically, fragment en masse from a larger podosome, the podosome cluster precursor (PCP). Based on the differential effects of microtubule inhibitors on podosome turnover, we suggest that the PCP is an important intermediate that generates new adhesions at the front of a cell.

Results and discussion

Podosomes adhere to the substratum

Podosomes have classic features of a focal complex. Each actin-rich podosome is short-lived and punctate, contains actin cross-linking proteins (Marchisio et al., 1987; Babb et al., 1997), and when imaged by interference reflection microscopy (IRM), is in close apposition to the substratum (Izzard and Lochner, 1976; Tarone et al., 1985). Because podosomes are dynamic structures, we first verified when podosomes acquire key characteristics of a focal complex. Two markers for adhesions are colocalization with integrins (Marchisio et al., 1988) and close proximity to the substratum (Izzard and Lochner, 1976). Immunofluorescence micrographs show that cd11c (αX integrin) and F-actin colocalize at podosomes. When reconstructed in three dimensions, distinct subregions containing integrins are visible in the larger actin-containing structures (Fig. 1, E and F). Furthermore, actin- and integrin-containing structures colocalized with regions in close proximity to the substratum (Fig. 1, C–F). The coincidence of actin, integrin, and IRM signals suggests that the majority of podosomes at the leading edge are involved in adhesion to the substratum.

Podosomes assemble, grow, and fragment

In live cells observed with phase optics, podosomes appear as small, phase-dense structures that continuously form at the periphery of the macrophage lamella (Video 1, available at http://www.jcb.org/cgi/content/full/jcb.200212037/DC1). When marked by GFP-tagged fimbrin or actin, podosomes appear and disappear within a few minutes at the leading lamella, confirming previous observations (Kanehisa et al., 1990). However, in addition to the rapid turnover of many podosomes, time-lapse microscopy showed the transient presence of a large amorphous fimbrin- and actin-containing structure immediately preceding the appearance of a cluster of four to six podosomes (Fig. 2 A). To identify the function of this structure more clearly, we imaged the entire axial volume of the macrophage lamella by three-dimensional (3-D) time-lapse (4-D) microscopy (Fig. 2 B and Video 2). In 3-D reconstructions, the volume of the large amorphous structure was 5–10-fold larger than individual podosomes (5–10 fL vs. 0.5–2 fL) and preceded podosomes by 1–2 min (Fig. 2 B and Video 3). The axial height of PCPs and podosomes was ∼1–2 μm (Fig. 2 C), a length sufficient to span the distance between dorsal and ventral plasma membranes in the lamella as measured previously by EM (Trotter, 1981; Kato and Akisaka, 1994). We termed the structure a podosome cluster precursor because it appeared to generate several new juxtaposed podosomes.

To visualize the precursor–product relationship of the PCP and podosomes, we analyzed 4-D images by kymography in which the position (x, y) and outline of the PCP was traced over time (t; Fig. 2 D). The kymograph showed the appearance of a single podosome, its steady growth in volume into a PCP, and fragmentation into a cluster of several daughter podosomes. The trace was continuous over 20 min and sloped, in a stepwise manner, toward the front of the advancing cell. This behavior suggests an assembly mechanism involving nascent assembly of a podosome, growth into a PCP, and fragmentation into several podosomes. Fragmentation has two benefits; it extends the lifetime of a podosome and rapidly generates multiple adhesion sites.

Podosome dynamics: measurement of lifetime and actin turnover

Analysis of a single podosome cluster implicated growth and fragmentation as a mechanism for the generation of new podosomes. To study the assembly mechanism in more detail, we developed algorithms for measuring key parameters of podosome dynamics; the lifetime and fission frequency of all podosomes in an imaged volume (x, y, t) of the cell. Because it is implicated in organizing actin in podosomes (Babb et al., 1997), we also analyzed the dynamics of the actin cross-linking protein fimbrin. Analysis of time-lapse movies (Fig. 3 A) showed that β-actin–ECFP and L-fimbrin–EYFP colocalized to the core of each podosome. In kymographs, fimbrin revealed a pattern of dynamics that was coincident in space and time to that of actin (Fig. 3 B). Kymograph traces from actin and fimbrin showed both short-lived and longer-lived branching structures. We were unable to detect any temporal difference in actin and fimbrin localization during assembly or turnover of podosomes. These observations suggest that actin and fimbrin are closely coupled dynamically in podosomes.

Branches in the kymographs showed qualitatively that podosomes may arise by fission of older podosomes. Using actin as a marker of podosomes, we quantified the assembly and turnover dynamics of the entire population of podosomes in the leading lamella by measuring their xy position and lifetime using kymographs (Fig. 4 A and Video 4). Analysis of kymographs revealed two podosome populations; short-lived "simple" and longer-lived "branched" podosomes. Simple podosomes correspond to the short tracks that assembled de novo and disappeared within a minute. In contrast, tracks of the majority of podosomes were long and continuous with average lifetimes of 7 min (Fig. 4, A and H).

Two types of kymograph branches were identified; fission events in which a trace split into two or more branches, and fusion events in which two branches merged. The fission pattern of assembly for branched podosomes is conceptually

*Abbreviations used in this paper: 2-, 3-, and 4-D, two, three, and four dimensional; IRM, interference reflection microscopy; PCP, podosome cluster precursor.

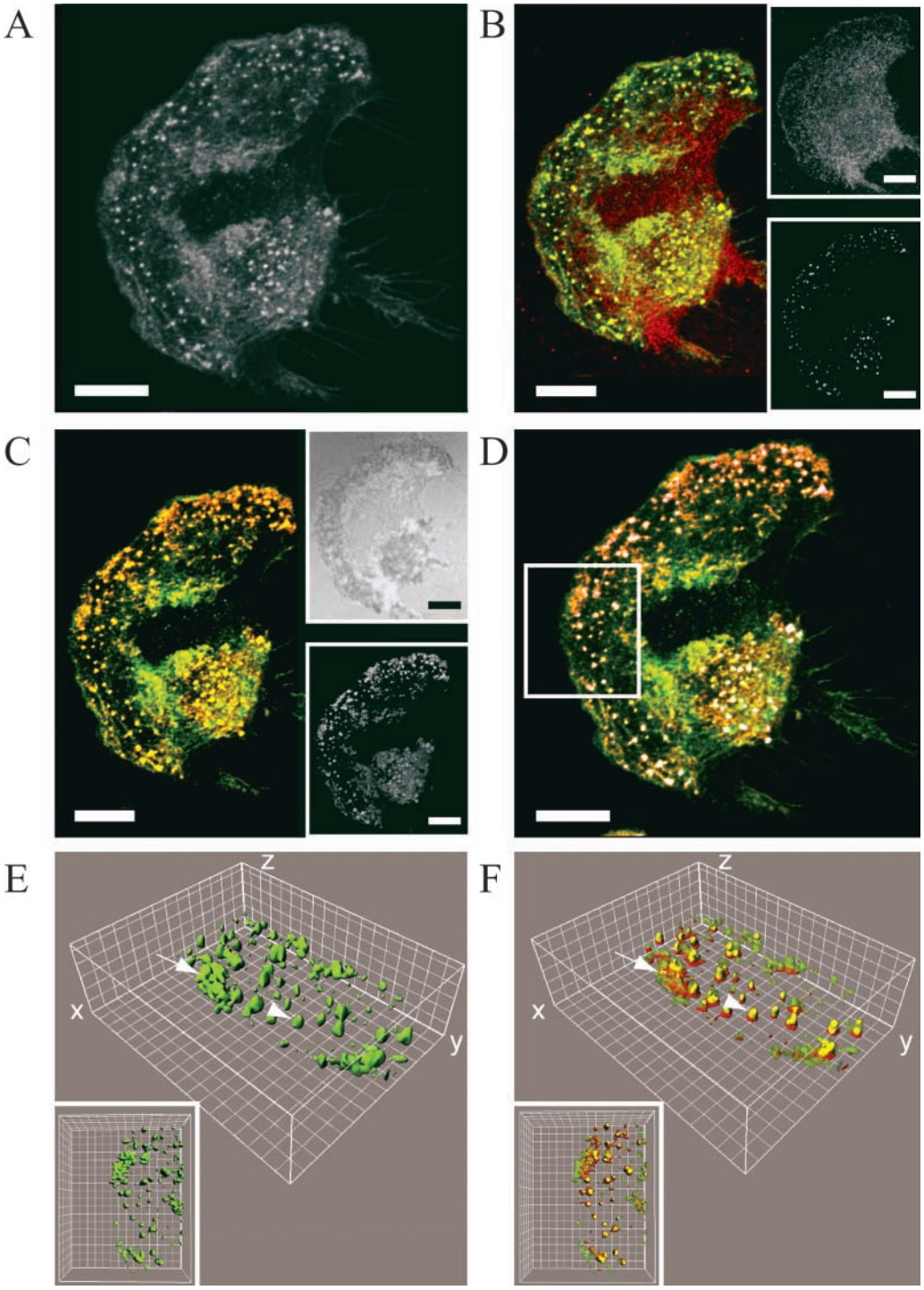

Figure 1. **Podosomes colocalize with integrins and are in close proximity to the substratum.** (A) Maximum intensity projection of phalloidin-FITC fluorescence showing distribution of F-actin in an IC-21 macrophage. (B) Overlay of phalloidin-FITC (green) and anti-cd11c fluorescence (red and top inset). 3-D colocalization (yellow and bottom inset) of the two channels predominantly at the leading edge and actin foci. (C) Proximity of podosomes to the substratum as shown by IRM (top inset). Colocalization (yellow and bottom inset) of phalloidin-FITC with the inverted IRM signal shows leading edge and podosome-containing regions in close proximity to the substratum. (D) Podosomes show a high correlation of integrin colocalization (blue, bottom inset in B) and substratum proximity (red, bottom inset in C) as indicated by the white signal of the majority of podosomes. Bars, 10 μm. (E and F) 3-D reconstruction of the boxed region in D shows that F-actin (green) is present in large (arrow) and small (arrowhead) podosomes, and that both are in close proximity to the substratum as shown by IRM (red) and contain integrin colocalization (yellow). Grid squares are 1 μm × 1 μm.

similar to kymograph traces of actin barbed ends in the dendritic actin network; both structures branch in the direction of lamellar extension (Video 5). Analysis of the podosome branching patterns showed that fission and fusion branches occur at similar rates (Fig. 4 H). Furthermore, new branches form toward the front of the cell to position daughter podosomes predominantly at the extending leading edge.

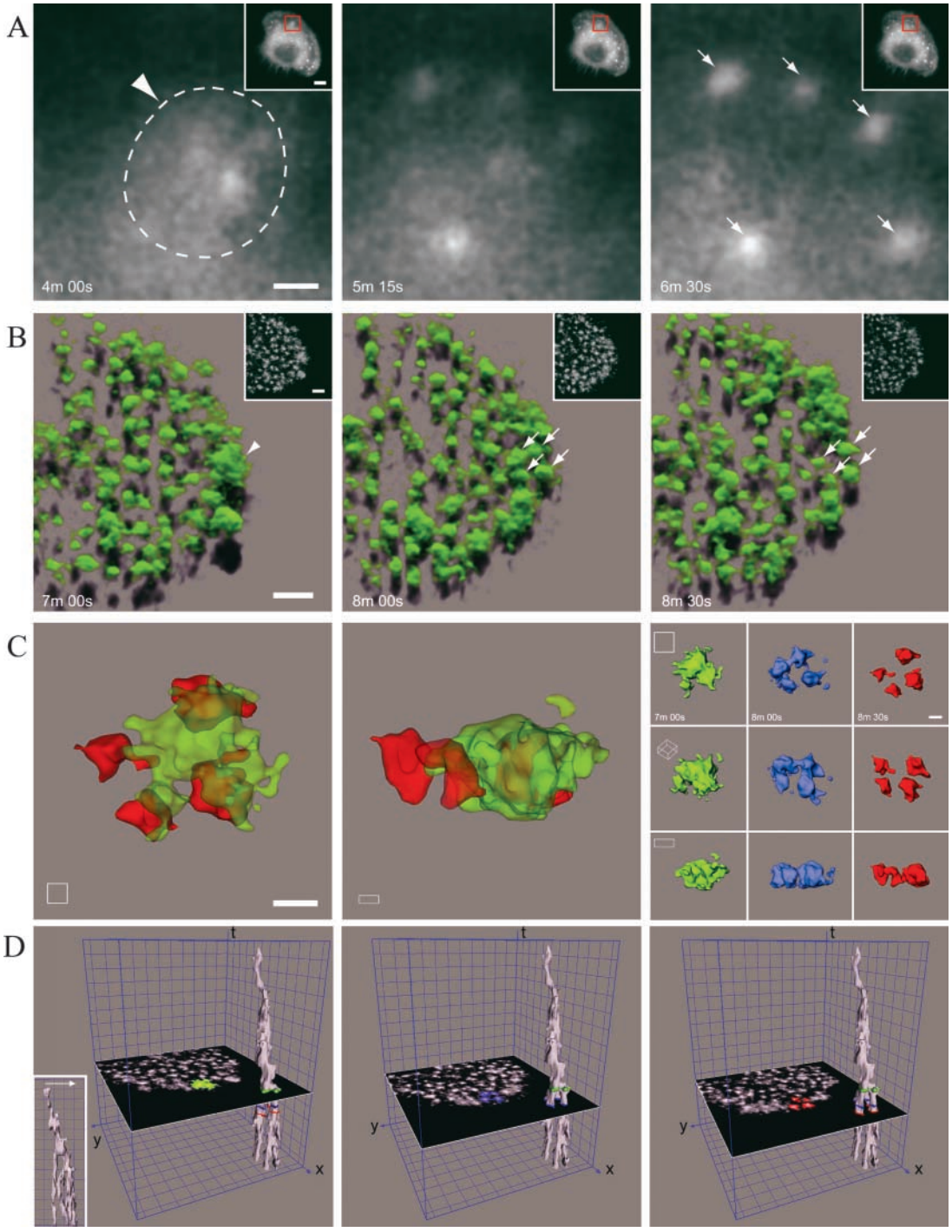

Figure 2. **Podosome clusters arise from PCPs.** (A) Frames from a 2-D wide-field time-lapse experiment showing L-fimbrin–EGFP fluorescence at the leading edge of an IC-21 macrophage. An amorphous area of fluorescence (PCP, dashed line and arrowhead) precedes a cluster of individual podosomes (arrows). Bar, 10 μm; 1 μm (inset). (B) In a 4-D experiment, SFP rendering of β-actin–EYFP fluorescence at the leading edge of an IC-21 macrophage shows a PCP (arrowhead) followed a few minutes later by a cluster of smaller, discrete podosomes (arrows). Deconvolved data were rendered with the SFP algorithm in which objects, illuminated from above, cast a shadow aiding visual perception of 3-D structures. Maximum intensity projections of the same data are shown in the insets (see Video 2) Bars, 3 μm. (C) XY (left) and XZ (middle) views of isosurface reconstructions showing that a podosome cluster (red) formed from a PCP (green). Panels on the right show color-coded time points (green the earliest, red the latest). Bar, 1 μm. (D) Podosome cluster formation visualized by maximum intensity projection of each 3-D time point and tracing the high intensity structures over time. In the kymograph (gray, offset in main panels, side view left panel inset), the PCP (green) is seen to assemble (long single trace) and then simultaneously form several new podosomes (branches, blue and red structures). Side projection of the kymograph (inset) follows the direction of lamellar extension (arrow). Grid squares are 2 μm (x, y) and 1 min (t).

In contrast to the anteriorly polarized formation of podosome clusters at the leading edge, simple podosomes are distributed throughout the leading lamella (Fig. 4 B). Interestingly, their short lifetime is similar to the mean lifetime of a daughter podosome (Fig. 4 H). This similarity suggests that podosome lifetime may be preset and

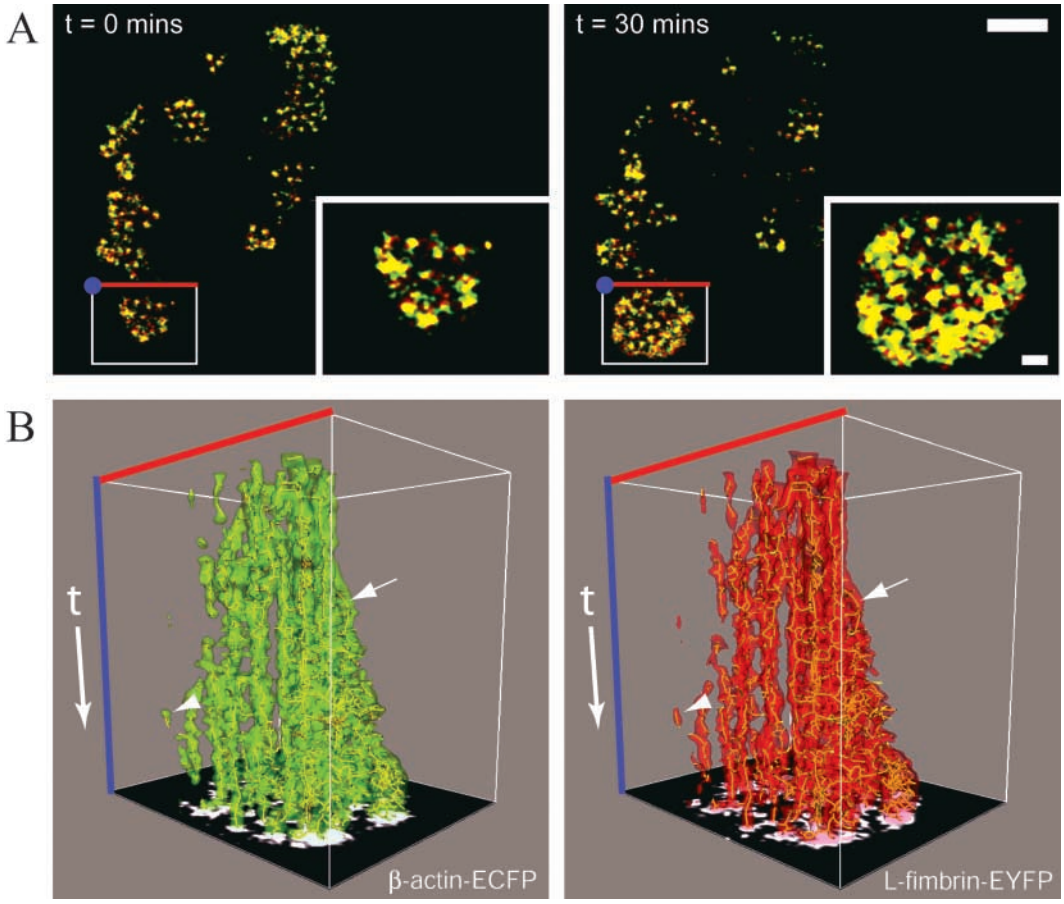

Figure 3. **Actin and fimbrin dynamics at the leading edge.** (A) 2-D time-lapse deconvolution confocal microscopy of β-actin–ECFP (green) and L-fimbrin–EYFP (red) recorded at 15-s intervals for 30 min. Colocalized signals are shown in yellow. Insets show the boxed region at higher magnification at t = 0 (left) and 30 min later (right). Bar, 10 μm. (B) Kymographs from the boxed region (A) shows that actin (left, green) and fimbrin (right, red) have similar lateral distribution over time producing short-lived traces (arrowhead) and longer-lived branching traces (arrow). A 2-D image of the last time point forms the floor of the kymograph box. The boxed region is 15 μm × 20 μm × 30 min.

only extended by other factors such as growth, fission, or fusion.

Because podosomes lie close to the dendritic actin network of the leading lamella, we investigated whether podosome lifetime was coupled to turnover of the actin subunit pool. We photobleached selected areas of the lamella and performed FRAP analysis. Fluorescence recovered completely in photobleached podosomes within 2 min and a half-time of ~20 s (Fig. 4, C and D), consistent with kymograph-based measurements of podosome lifetime and confirming the high rate of actin turnover in these structures (Ochoa et al., 2000). FRAP appeared uniform across the photobleached region, showing no preference for a subpopulation of podosomes based on size or location. Disruption of actin turnover by either sequestration of monomers using latrunculin A or stabilization of filaments using jasplakinolide had the expected result of inhibiting FRAP (Fig. 4 C; Ochoa et al., 2000). These results suggest that actin constantly turns over at similar rates in both simple and branched podosomes.

Regulation of podosome assembly by microtubules

Fragmentation and fusion of podosomes are novel mechanisms for assembly of adhesions. Because microtubules have been implicated in the assembly of cell adhesions and the actin cytoskeleton (Babb et al., 1997; Elbaum et al., 1999; Kaverina et al., 1999; Linder et al., 1999), we investigated whether microtubules influenced podosome assembly dynamics. In a preliminary work, we confirmed that podosomes contain a core of bundled actin filaments oriented perpendicularly to the substratum by EM (Trotter, 1981), and documented the close proximity of podosomes with microtubules (Fig. 4 E). All podosomes had an associated microtubule; either many podosomes distributed along the length of a single microtubule or a podosome intersected by several microtubules. When microtubules were stabilized with paclitaxel or destabilized with demecolcine, persistent cell motility ceased but podosomes remained intact (Fig. S1). The stability of podosomes was not caused by a decrease in the rate of actin turnover, as FRAP after paclitaxel and demecolcine treatment was identical to that in untreated cells (Fig. 4 C). Because several reports have suggested that microtubule interactions may increase the stability of short-lived adhesions (Kaverina et al., 1999; Linder et al., 2000), we analyzed kymographs of microtubule-perturbed cells and found a clear qualitative difference in the stability of branched podosomes, but no effect on simple podosomes (Fig. 4, F and G). Demecolcine shortened branched podo-

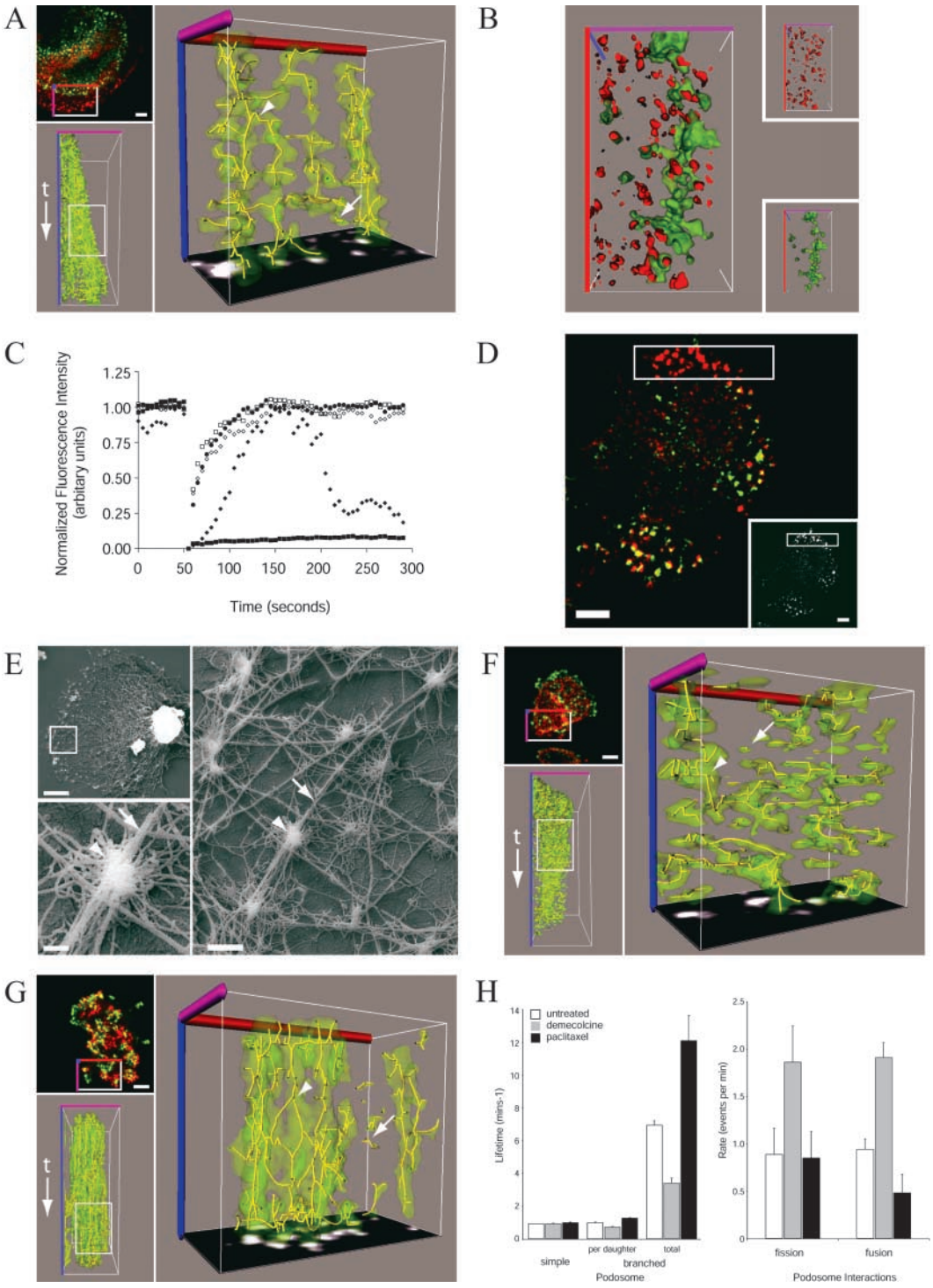

Figure 4. **Quantitative analysis of podosome assembly.** (A) 2-D images of β-actin–EYFP fluorescence recorded by deconvolution confocal microscopy at 15-s intervals for 30 min. The top inset compares β-actin–EYFP fluorescence at t = 0 (green) and t = 30 (red) Bar, 3 μm. An x, y, t (red, purple, blue) boxed area (17.9 μm × 9.8 μm × 28.25 min) was analyzed by kymography. Side projections (bottom inset) of the kymograph show that the leading edge extends in the y-direction (purple axis) over time (blue axis). The boxed region in the bottom inset shows the position of the subregion (8.45 μm × 4.85 μm × 8.25 min) shown in the main panel. The kymograph displays the time-dependent location of podosomes as a centroid (yellow line) and volume (transparent green). Short-lived podosomes (arrows) and branched podosomes (arrowheads) are present. A 2-D image of the last time point forms the floor of the kymograph box (Video 3). (B) Branched podosomes (green) are primarily present at the extreme leading edge, whereas simple podosomes (red) are present throughout the leading edge adhesion zone (~5 μm). The x, y, t volume (red, purple, blue) measures 17.9 μm × 9.8 μm × 5 min with the leading edge facing right. (C) In untreated macrophages, β-actin–EYFP FRAP occurred with a half time of 21.37 ± 3.26 s (filled circles, $n = 7$). No FRAP occurred in cells treated with jasplakinolide (filled squares, $n = 8$). Latrunculin A treatment did not prevent FRAP until podosomes were completely disassembled (filled diamonds, $n = 8$). Paclitaxel- and demecolcine-treated cells recovered fluorescence at similar rates to controls 21.24 ± 3.22 s (open squares,

Figure 4 legend continued on next page.

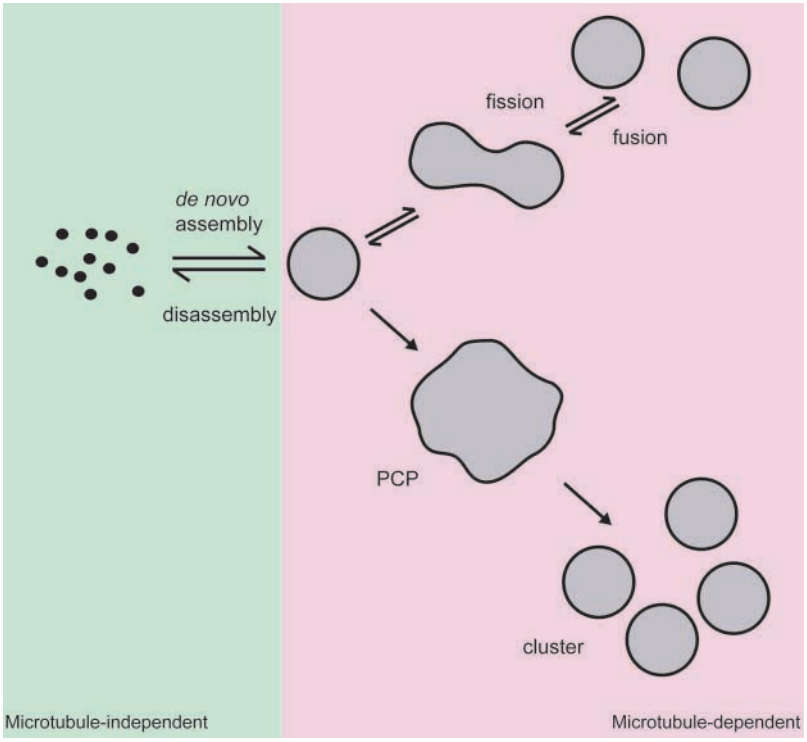

Figure 5. **A model for podosome assembly.** Podosome assembly and disassembly takes place within an adhesion-rich zone. At the leading edge of the lamella, a podosome assembles de novo and disassembles in a microtubule-independent process. Podosome lifetime can be extended in a microtubule-dependent process by fission into daughter podosomes, fusion with another podosome, or growth into a PCP and fission into a podosome cluster. The assembly of daughter podosomes keeps pace with the leading lamella, whereas the mother podosome remains stationary until disassembling at the rear of the adhesion zone.

some lifetime, but when microtubules were stabilized with paclitaxel, the total lifetime of branched podosomes increased. Kymograph quantitation (Fig. 4 H) revealed that the mean lifetime of daughter podosomes was either decreased or increased by ~25% when microtubules were perturbed with demecolcine or paclitaxel, respectively. The small changes in longevity of individual daughter podosomes were additive over time, leading to an ~50% change in the mean lifetime of branched podosomes. Podosome assembly and turnover continued despite a lack of persistent leading edge extension, demonstrated by an absence of lateral progression in kymographs from demecolcine- and paclitaxel-treated cells (Fig. 4, F and G).

Because the lifetime of branched podosomes is dependent on the fusion and fission between podosomes, we investigated the effects of microtubule stability on the interactions between adjacent podosomes (Fig. 4 H). After microtubule destabilization, a twofold increase in the rates of fusion and fission events was measured. However, when microtubules were stabilized, the fusion rates decreased but the fission rates remained unchanged from controls. Changes in branching rates after microtubule disruption suggests that fusion and fission of podosomes are not random events occurring steadily over time. On the contrary, these observations suggest an active mechanism involving microtubules in the physical separation and aggregation of podosomes.

A model for polarized assembly of podosomes at the leading edge

Our analysis of podosome assembly and turnover reveals a growth and fragmentation pattern of cell adhesion assembly that positions new adhesions at the very front of the cell. Podosomes are similar to the short-lived precursors of focal adhesions, focal complexes which, like actin-rich membrane ruffles at the leading edge, are maintained by Rac activity associated with the presence of dynamic microtubules (Rottner et al., 1999; Waterman-Storer et al., 1999). Time-lapse analyses show that focal complexes assemble at the leading edge (Rottner et al., 1999), "maturing" into larger elongated stationary focal adhesions in response to elevated Rho activity until being disassembled in a perinuclear culling zone as the cell moves forward (Smilenov et al., 1999). Podosomes in moving macrophages are also confined to the periphery of the leading edge, but are disassembled outside of this zone.

n = 8) and 16.38 ± 2.57 s (open diamonds, n = 8), respectively. Representative plots for each treatment are shown. (D) Selected frames of deconvolved β-actin–EYFP fluorescence from an untreated IC-21 macrophage immediately before (inset) and after photobleaching (green), and ~2 min later (red). Green and red images are overlaid so that FRAP within the photobleached region (boxed) is indicated in red. Bar, 5 μm. (E) EM analysis of a detergent-extracted IC-21 macrophage. Podosomes (arrowhead) appeared in close proximity to microtubules (arrow) throughout the leading lamella. At higher magnification, microtubules (arrow) appeared to pass over or next to the tightly bundled podosome core (arrowhead). Bars: 5 μm (top inset), 500 nm (main panel), and 200 nm (bottom inset). (F and G) Kymographs from IC-21 macrophages treated with either 1 μM demecolcine for 5 min (F) or 10 μM paclitaxel for 45 min (G). Simple (arrows) and branched podosomes (arrowheads) are present in F and G, but traces appear shorter after demecolcine treatment and longer after paclitaxel treatment, compared with untreated cells (A). All dimensions as indicated for A. (H) Quantitation of centroid trace lengths expressed as the mean lifetime of podosomes from untreated (n = 5), demecolcine-treated (n = 5), and paclitaxel-treated (n = 5) cells for simple and branched podosomes (left). Branched podosome lifetime is shown per daughter (i.e., branch) and for the total length (from appearance of first daughter until disassembly of last daughter). The fusion and fission events (right) were identified and expressed as a rate (events/min).

We speculate that in order to escape disassembly of the actin bundles, fusion and fission events enable podosomes to "step away" from the disassembly zone and toward the Rac-dependent dendritic actin network at the leading edge. The direction of podosome stepping may be influenced by physical interaction with microtubules involving Wiskott-Aldrich syndrome protein and its effector Cdc42 interacting protein-4 (Linder et al., 2000). In growth cones and the leading lamella, microtubules "steer" the direction of cell motility by influencing the stability of the actin cytoskeleton and cell adhesions (Tanaka and Kirschner, 1995; Buck and Zheng, 2002; Zhou et al., 2002). Although the exact molecular mechanism regulating fusion and fission of adhesions remains elusive, our results indicate that microtubules not only influence adhesion longevity, but also influence the mobility and interaction of cell adhesions.

To provide a framework for understanding podosome dynamics, we have developed a model for the assembly and turnover of podosomes (Fig. 5). At the leading edge, podosomes assemble de novo and are stabilized in a microtubule-dependent manner leading to fusion with a neighboring podosome, fission into daughter podosomes, or more dramatically, growth into a PCP and fission into a podosome cluster (Fig. 4). Not only is the PCP a novel adhesion-related structure, but repeated fusion and fission of podosomes is also a novel mode of behavior for nonmembrane-bound supramolecular structures. These processes supply new podosomes at the leading edge of the cell as it advances. The significance of this non-de novo assembly mechanism may be the ability of podosomes to transfer tension from an existing site to a nascent site, thus pulling the lamella forward as the leading edge extends.

Materials and methods

Cell culture

IC-21 macrophages (TIB-186; American Type Culture Collection) were cultured as described previously (Correia et al., 1999). Pantropic constructs (CLONTECH Laboratories, Inc.) were used for stable expression of moderate levels of GFP protein fusions. Virus–cell interaction was promoted using RetroNectin™-coated plates (Takara Bio, Inc.). Macrophages were stimulated by incubation in media containing 100 ng/ml lipopolysaccharide and 300 U/ml interferon-γ (Sigma-Aldrich) for 16 h before observation. For microtubule destabilization, cells were incubated in media with 1 μM demecolcine (ICN Biomedicals) for 15–30 min. Microtubules were stabilized by 10 μM paclitaxel (Sigma-Aldrich) for 45–75 min. Actin monomers were sequestered by 200 nM latrunculin A (Sigma-Aldrich), and actin polymerization was promoted by 10 μM jasplakinolide (Molecular Probes, Inc.).

Light and electron microscopy

IC-21 macrophages were maintained at 37°C using a heated microscope stage (Carl Zeiss MicroImaging, Inc.) and an objective heater (Bioptechs). Fluorescence was measured using a confocal microscope (LSM510 META; Carl Zeiss MicroImaging, Inc.). To limit photobleaching, the 25-mW argon laser was used at 0.2–3% and maximum scan speed. For ECFP/EYFP imaging, also using the confocal microscope (LSM510 META; Carl Zeiss MicroImaging, Inc.), a 560LP filter was used to eliminate ECFP bleed-through. For two-dimensional (2-D) time-lapse experiments, images were collected with 80–100 nm sampling and 2.5-s intervals for FRAP analyses, or 15-s intervals for tracking experiments. Photobleaching was achieved by scanning a subregion 40 times with 458-nm, 488-nm, 514-nm, 543-nm, and 633-nm laser lines at maximum power, lasting 3 s. 4-D data were collected at 90 nm XY and 100 nm Z intervals (voxel volume of 0.81 aL) over an axial distance of 4–5 μm with 30-s intervals between each stack. Cells were fixed and stained as described previously (Correia et al., 1999). Anti-cd11c (DakoCytomation) was used at 1:50. Confocal IRM used the 633-nm laser with a 628–638 nm emission filter (Izzard and Lochner, 1976).

For EM, a modification of the method described by Svitkina and Borisy (1998) was used. Cells were rinsed briefly in PEM-light buffer (80 mM Pipes, pH 7.1, 5 mM EGTA, pH 7.1, and 2 mM $MgCl_2$) and extracted for 5 min at 26°C in PEM buffer (100 mM Pipes, pH 7.1, 2 mM EGTA, pH 7.1, and 2 mM $MgCl_2$) with 1% Triton X-100 (Pierce Chemical Co.), 4 μM phalloidin (Molecular Probes, Inc.), and 10 μg/ml paclitaxel (Sigma-Aldrich). Extracted cells were rinsed in detergent-free buffer and fixed before critical-point drying and rotary shadowing with 1–3 nm platinum. For transmission images of carbon-coated platinum replicas, a microscope was used (model EM410; Philips).

Image processing and analysis

Images were deconvolved using Huygens2 (Scientific Volume Imaging). FRAP analyses used Huygens2 and Origin® software version 6.1 (OriginLab Corporation). Podosome tracking and half-life analyses were performed using NeuronTracer (Bitplane), Imaris3 (Bitplane), and Origin® software version 6.1. Perl scripts assembled and grouped object data from NeuronTracer and Huygens2. IRM images were Gaussian filtered at twice the sampling frequency to reduce noise before colocalization using Imaris3. 4-D data were rendered and volumes were calculated using Imaris3. Statistical analyses used Excel (Microsoft) and Origin® software version 6.1. Videos were generated using HyperCam™ (Hyperionics) and Flash 5 (Macromedia). Figures were assembled using Adobe Illustrator®.

Online supplemental material

Fig. S1 shows transmission EM images of detergent-extracted macrophages after cytoskeletal disruption, and immunogold staining for fimbrin in podosomes. Video 1 contains time-lapse microscopy using phase optics showing IC-21 macrophage motility. Video 2 contains 4-D microscopy showing the formation and turnover of podosomes at the leading edge of an IC-21 macrophage expressing β-actin–EYFP. Video 3 shows an isosurface reconstruction of a PCP at the leading edge of an IC-21 macrophage expressing β-actin-EYFP. Video 4 shows 3-D tracking of podosomes at the leading edge of an IC-21 macrophage expressing β-actin–EYFP. Video 5 shows kymograph tracking of barbed ends during simulated polymerization of a branched actin filament network. Online supplemental material available at http://www.jcb.org/cgi/content/full/jcb.200212037/DC1.

Thanks to S. Ray, M. Messerli, H. van der Voort, and B. Yuan for help with image analysis software and hardware. We thank B. Chen, F. Gertler, C. Hug, R. Hynes, D. Lauffenburger, and J. Newman for helpful comments during manuscript preparation. All images were collected and processed at the WM Keck Facility for Biological Imaging and the Whitehead Institute/Massachusetts Institute of Technology BioImaging Center.

This work was supported by a grant from the National Institutes of Health (GM57418).

Submitted: 4 December 2002
Revised: 31 March 2003
Accepted: 1 April 2003

References

Babb, S.G., P. Matsudaira, M. Sato, I. Correia, and S.S. Lim. 1997. Fimbrin in podosomes of monocyte-derived osteoclasts. *Cell Motil. Cytoskeleton.* 37:308–325.

Beningo, K.A., M. Dembo, I. Kaverina, J.V. Small, and Y.L. Wang. 2001. Nascent focal adhesions are responsible for the generation of strong propulsive forces in migrating fibroblasts. *J. Cell Biol.* 153:881–888.

Buck, K.B., and J.Q. Zheng. 2002. Growth cone turning induced by direct local modification of microtubule dynamics. *J. Neurosci.* 22:9358–9367.

Correia, I., D. Chu, Y.H. Chou, R.D. Goldman, and P. Matsudaira. 1999. Integrating the actin and vimentin cytoskeletons, adhesion-dependent formation of fimbrin-vimentin complexes in macrophages. *J. Cell Biol.* 146:831–842.

Elbaum, M., A. Chausovsky, E.T. Levy, M. Shtutman, and A.D. Bershadsky. 1999. Microtubule involvement in regulating cell contractility and adhesion-dependent signalling: a possible mechanism for polarization of cell motility. *Biochem. Soc. Symp.* 65:147–172.

Geiger, B., and A. Bershadsky. 2001. Assembly and mechanosensory function of focal contacts. *Curr. Opin. Cell Biol.* 13:584–592.

Geiger, B., Z. Avnur, G. Rinnerthaler, H. Hinssen, and V.J. Small. 1984. Microfilament-organizing centers in areas of cell contact: cytoskeletal interactions

during cell attachment and locomotion. *J. Cell Biol.* 99:83s–91s.

Izzard, C.S., and L.R. Lochner. 1976. Cell-to-substrate contacts in living fibroblasts: an interference reflexion study with an evaluation of the technique. *J. Cell Sci.* 21:129–159.

Kanehisa, J., T. Yamanaka, S. Doi, K. Turksen, J.N. Heersche, J.E. Aubin, and H. Takeuchi. 1990. A band of F-actin containing podosomes is involved in bone resorption by osteoclasts. *Bone.* 11:287–293.

Kato, T., and T. Akisaka. 1994. The cytoskeletal framework of chick osteoclasts in resin-less sections. *J. Anat.* 185:599–607.

Kaverina, I., O. Krylyshkina, and J.V. Small. 1999. Microtubule targeting of substrate contacts promotes their relaxation and dissociation. *J. Cell Biol.* 146: 1033–1044.

Lauffenburger, D.A., and A.F. Horwitz. 1996. Cell migration: a physically integrated molecular process. *Cell.* 84:359–369.

Linder, S., D. Nelson, M. Weiss, and M. Aepfelbacher. 1999. Wiskott-Aldrich syndrome protein regulates podosomes in primary human macrophages. *Proc. Natl. Acad. Sci. USA.* 96:9648–9653.

Linder, S., K. Hufner, U. Wintergerst, and M. Aepfelbacher. 2000. Microtubule-dependent formation of podosomal adhesion structures in primary human macrophages. *J. Cell Sci.* 113:4165–4176.

Marchisio, P.C., D. Cirillo, A. Teti, A. Zambonin-Zallone, and G. Tarone. 1987. Rous sarcoma virus-transformed fibroblasts and cells of monocytic origin display a peculiar dot-like organization of cytoskeletal proteins involved in microfilament-membrane interactions. *Exp. Cell Res.* 169:202–214.

Marchisio, P.C., L. Bergui, G.C. Corbascio, O. Cremona, N. D'Urso, M. Schena, L. Tesio, and F. Caligaris-Cappio. 1988. Vinculin, talin, and integrins are localized at specific adhesion sites of malignant B lymphocytes. *Blood.* 72: 830–833.

Mizutani, K., H. Miki, H. He, H. Maruta, and T. Takenawa. 2002. Essential role of neural Wiskott-Aldrich syndrome protein in podosome formation and degradation of extracellular matrix in src-transformed fibroblasts. *Cancer Res.* 62:669–674.

Ochoa, G.C., V.I. Slepnev, L. Neff, N. Ringstad, K. Takei, L. Daniell, W. Kim, H. Cao, M. McNiven, R. Baron, and P. De Camilli. 2000. A functional link between dynamin and the actin cytoskeleton at podosomes. *J. Cell Biol.* 150: 377–389.

Pfaff, M., and P. Jurdic. 2001. Podosomes in osteoclast-like cells: structural analysis and cooperative roles of paxillin, proline-rich tyrosine kinase 2 (Pyk2) and integrin alphaVbeta3. *J. Cell Sci.* 114:2775–2786.

Reinhard, M., M. Halbrugge, U. Scheer, C. Wiegand, B.M. Jockusch, and U. Walter. 1992. The 46/50 kDa phosphoprotein VASP purified from human platelets is a novel protein associated with actin filaments and focal contacts. *EMBO J.* 11:2063–2070.

Ridley, A.J., H.F. Paterson, C.L. Johnston, D. Diekmann, and A. Hall. 1992. The small GTP-binding protein rac regulates growth factor-induced membrane ruffling. *Cell.* 70:401–410.

Rottner, K., A. Hall, and J.V. Small. 1999. Interplay between Rac and Rho in the control of substrate contact dynamics. *Curr. Biol.* 9:640–648.

Smilenov, L.B., A. Mikhailov, R.J. Pelham, E.E. Marcantonio, and G.G. Gundersen. 1999. Focal adhesion motility revealed in stationary fibroblasts. *Science.* 286:1172–1174.

Svitkina, T.M., and G.G. Borisy. 1998. Correlative light and electron microscopy of the cytoskeleton of cultured cells. *Methods Enzymol.* 298:570–592.

Tanaka, E., and M.W. Kirschner. 1995. The role of microtubules in growth cone turning at substrate boundaries. *J. Cell Biol.* 128:127–137.

Tarone, G., D. Cirillo, F.G. Giancotti, P.M. Comoglio, and P.C. Marchisio. 1985. Rous sarcoma virus-transformed fibroblasts adhere primarily at discrete protrusions of the ventral membrane called podosomes. *Exp. Cell Res.* 159:141–157.

Trotter, J.A. 1981. The organization of actin in spreading macrophages. The actin-cytoskeleton of peritoneal macrophages is linked to the substratum via transmembrane connections. *Exp. Cell Res.* 132:235–248.

Volberg, T., B. Geiger, Z. Kam, R. Pankov, I. Simcha, H. Sabanay, J.L. Coll, E. Adamson, and A. Ben-Ze'ev. 1995. Focal adhesion formation by F9 embryonal carcinoma cells after vinculin gene disruption. *J. Cell Sci.* 108:2253–2260.

Volkman, B.F., K.E. Prehoda, J.A. Scott, F.C. Peterson, and W.A. Lim. 2002. Structure of the N-WASP EVH1 domain-WIP complex: insight into the molecular basis of Wiskott-Aldrich Syndrome. *Cell.* 111:565–576.

Waterman-Storer, C.M., R.A. Worthylake, B.P. Liu, K. Burridge, and E.D. Salmon. 1999. Microtubule growth activates Rac1 to promote lamellipodial protrusion in fibroblasts. *Nat. Cell Biol.* 1:45–50.

Zamir, E., M. Katz, Y. Posen, N. Erez, K.M. Yamada, B.Z. Katz, S. Lin, D.C. Lin, A. Bershadsky, Z. Kam, and B. Geiger. 2000. Dynamics and segregation of cell-matrix adhesions in cultured fibroblasts. *Nat. Cell Biol.* 2:191–196.

Zhou, F.Q., C.M. Waterman-Storer, and C.S. Cohan. 2002. Focal loss of actin bundles causes microtubule redistribution and growth cone turning. *J. Cell Biol.* 157:839–849.